NUMERICAL SIMULATION OF INTERNAL COMBUSTION ENGINES FUELLED BY NATURAL GAS

Dalton Bertoldi, dalton@polo.ufsc.br
Programa de Pós-Graduação em Engenharia Mecânica
Universidade Federal de Santa Catarina
88040-900, Florianópolis, SC, Brazil

César J. Deschamps, deschamps@polo.ufsc.br
Amir A. M. Oliveira Jr., amir@emc.ufsc.br
Departamento de Engenharia Mecânica
Universidade Federal de Santa Catarina
88040-900, Florianópolis, SC, Brazil

Abstract. *The increasing interest for less polluting energy sources has motivated the use of natural gas as an alternative fuel for internal combustion engine vehicles. The present paper addresses the development of a two-dimensional numerical model to simulate a spark-ignition engine fuelled by a stoichiometric mixture of air and methane. The main objective is the analysis of physical phenomena related to the in-cylinder fluid dynamics, heat transfer and combustion. In this respect, results are provided for velocity, turbulence intensity, temperature and pressure fields. The effects of the engine operation parameters on the engine performance is assessed through predictions of indicated power, torque and specific fuel consumption as well as volumetric and thermal efficiencies.*

Keywords*: internal combustion engine, natural gas*

1. INTRODUCTION

Natural gas is a widely used alternative fuel for internal combustion engines, both in automotive and stationary power generation. From fossil fuels, natural gas has, in average, the largest hydrogen-to-carbon ratio. In this respect, for the same amount of energy provided, natural gas emits the lowest amount of carbon dioxide from fossil fuel combustion. Das *et al.* (2000) show that, in a comparison to gasoline, natural gas emits 15% less CO_2 for the same amount of heat produced. Also, Akansu *et. al* (2004) mention the excellent properties of the natural gas fuel, besides its large worldwide reserves, estimated in 1.498×10^{14} m^3.

Because of the aforementioned advantages, many studies have addressed the use of natural gas as an alternative fuel for internal combustion engines. Among many experimental studies, Johansson *et al.* (1995) have investigated experimentally the use of different types of cylinder heads for natural gas engines. Das *et al.* (2000) conducted a comparative investigation between compressed natural gas and hydrogen fueled engines in terms of thermal efficiency, mean effective pressure and specific fuel consumption for a four-stroke mono-cylinder engine. The results showed that the brake specific fuel consumption is reduced and brake thermal efficiency improved when hydrogen is used. Use with compressed natural gas resulted in 27.59% thermal efficiency, while use with hydrogen resulted in a 31.19% brake thermal efficiency.

Numerical simulations have also been developed addressing several issues. Among many others, Cartellieri *et al.* (1994) investigated numerically the fluid dynamics and combustion of a 9.6 liters internal combustion engine working with three different types of cylinder head. The results showed the influence of the mean velocity, turbulent kinetic energy, and other parameters on the overall engine performance. Zhang *et al.* (1998) investigated the effect of swirl, combustion chamber geometry and spark-plug location on the combustion rate and overall performance of a 2.2 and a 4.3 liters engine. The numerical results were compared to measurements and a good agreement was found. Thobois *et al.* (2003) analyzed numerically using a two-dimensional axisymmetric simulation, an engine operating with three different compositions of natural gas and also with iso-octane. The authors used correlations for the natural gas laminar flame speed to obtain the performance of a 1,750 cm^3 engine working with two different compression rates. Among the results obtained are combustion rate, in-cylinder pressure, turbulence intensity and indicated mean effective pressure.

The main goal of this work is to simulate numerically a small size spark-ignited internal combustion engine fuelled by natural gas. Methane gas is the major component of natural gas and more than 90% in volume of natural gas in Brazil and other countries is methane (Weaver, 1989). Since the low heating value of methane is similar to other hydrocarbons, the assumption of modeling natural gas as methane is a good approximation from the energy release point of view. However, it must be emphasized that small additions of larger hydrocarbons have a strong effect on the ignition behavior of natural gas (Westbrook *et al.*, 2005). Here, natural gas is modeled as pure methane and the ignition is treated through a simplified model, which does not take into account the presence of other constituents. A two-dimensional axisymmetric model is used and the full set of transient conservation equations for mass, momentum, energy and mass of chemical species is solved. A k-ε model is used for turbulence and an eddy-dissipation concept is used to model the methane combustion. The engine block is assumed isothermal and the engine is assumed to admit and

discharge in constant pressure plenums. The commercial code Fluent (Fluent Inc., 2006) is used for the numerical solutions. The numerical predictions are compared to other results available in the literature.

2. PROBLEM FORMULATION

2.1. Geometry

The main cylinder dimensions and other engine characteristics are listed in Table 1. The model for the intake, cylinder and exhaust systems rely on an axisymmetric two-dimensional approximation. In this model, the intake and exhaust valves are aligned with the axis of the cylinder. Both the cylinder and piston heads are plane and parallel. The intake aperture is positioned in the cylinder head, while the exhaust aperture is positioned in the piston head. The piston surface moves following a path prescribed by the crank axis rotation. The intake and exhaust valves move following prescribed polynomial functions, which model a fixed valve command. The spark plug is located in the center of the intake valve surface. Intake and exhaust valves are connected to constant pressure reservoirs (*plenum*). An intake plenum, the intake valve runner, the intake valve aperture, the cylinder, the exhaust valve aperture, the exhaust valve runner and the exhaust plenum then form the computational domain. Figure 1 shows a rendering of the computational domain.

Table 1. Main cylinder dimensions and other engine characteristics.

Bore	B	79.5 mm	Compression ratio	r	10:1
Stroke	L	80.5 mm	Displacement	V_d	0.4 cm^3
Connecting rod length	a	129.025 mm	Valves diameter	D	30.0 mm
Crank radius	R	40.25 mm	Valves lift	l	10.0 mm

This is an overly simplified model in terms of geometry even when compared to a laboratory engine. However, the model reproduces the main aspects that define the flow, reaction and heat transfer in an internal combustion engine. The valve runner and aperture, with the periodic motion of the valve surface reproduces the flow conditions at intake and exhaust in an internal combustion engine. The flow accelerates during intake and produces swirl and tumble movements of the charge inside the cylinder during admission. Once the valves are closed, the piston movement compresses the mixture and the spark-plug reproduces a central spark in the combustion chamber. Piston movement is allowed during expansion producing the expansion work. Once the exhaust valve is opened, blowdown and scavenging exhaust are reproduced. Then, the model, as it will be shown, reproduces the main aspects of fluid mechanics, combustion and heat transfer during engine operation being able to recover, in a fundamental level, the effects of engine operation parameters in performance. The major advantage of assuming the axisymmetric model is the reduction of computational time when compared to a fully three-dimensional model. This allows for the modeler to run fast a large number of simulations. The time spent in each simulation will be discussed later. Finally it is worth nothing that extension to a more geometrically realistic three-dimensional model is just a mater of defining the geometry, deploying grid and using more computational power and CPU time.

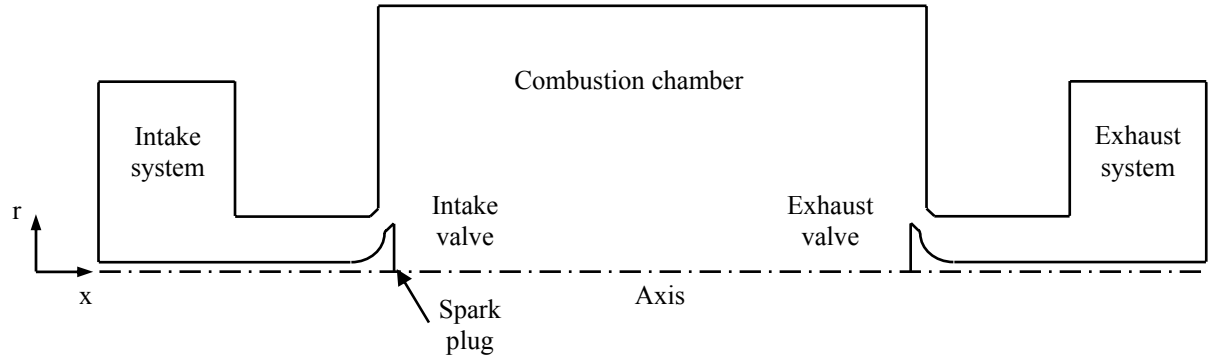

Figure 1. Rendering of the domain for the numerical simulations.

2.2. Governing equations

The chemical reaction is modeled as a global, one-step, chemical kinetic mechanism, with five chemical species. The mechanism, presented in Eq. (1) for a stoichiometric combustion of methane with standard dry air, describes methane oxidation to create carbon dioxide and water vapor. Nitrogen is assumed inert.

$$CH_4 + 2(O_2 + 3{,}76N_2) \rightarrow CO_2 + 2H_2O + 7{,}52N_2 \quad (1)$$

The fluid dynamic, for an inertial frame of reference, is modeled with the conservation equations of mass and momentum coupled with the conservation equations for thermal energy and mass of chemical species and a state equation for the gas (ideal gas behavior is assumed). Turbulence is modeled using the eddy viscosity concept through transport equations for the turbulent kinetic energy and the rate of viscous dissipation. The conservation equations are written in terms of Reynolds averages for ρ and p and Favre averages for the other variables (Peters, 2000). Here, for convenience, the average notation is suppressed in the conservation equations. The equation for conservation of mass is:

$$\frac{\partial \rho}{\partial t} + \frac{\partial \rho U_i}{\partial x_i} = 0 \tag{2}$$

where ρ is the specific mass and U is the velocity vector.

The conservation equation for the linear momentum, neglecting body forces, is written as:

$$\frac{\partial \rho U_i}{\partial t} + \frac{\partial \rho U_i U_j}{\partial x_j} = -\frac{\partial P}{\partial x_i} + \frac{\partial}{\partial x_j}\left(\mu \frac{\partial U_i}{\partial x_j} - \rho \overline{u'_i u'_j} \right) \tag{3}$$

where P is the pressure, μ is the molecular dynamic viscosity and $\rho \overline{u'_i u'_j}$ is the Reynolds stress tensor, which can be modeled according to:

$$\rho \overline{u'_i u'_j} = \mu_t \left(\frac{\partial U_i}{\partial x_j} + \frac{\partial U_j}{\partial x_i} \right) - \frac{2}{3}\delta_{ij}\left(\mu_t \frac{\partial U_\ell}{\partial x_\ell} + \rho k \right) \tag{4}$$

where μ_t is the turbulent viscosity and k is the kinetic energy.

The conservation equation for the mass of the chemical species i is written as:

$$\frac{\partial}{\partial t}(\rho Y_i) + \frac{\partial}{\partial x_j}(\rho Y_i U_j) = \frac{\partial}{\partial x_j}\left[\rho D_{i,m} \frac{\partial Y_i}{\partial x_j} - \rho \overline{y'_i u'_j} \right] + R_i \tag{5}$$

where Y_i is the mass fraction of species i, $D_{i,m}$ is the molecular diffusion coefficient for species i in the mixture and R_i is the species production rate *by* chemical reaction. The species turbulent flux in Eq. (5) is modeled according to:

$$-\rho \overline{y'_i u'_j} = \frac{\mu_t}{Sc_t} \frac{\partial Y_i}{\partial x_j} \tag{5}$$

where Sc_t is the Schmidt turbulent number.

The conservation equation for the thermal energy is given by:

$$\begin{aligned} &\frac{\partial}{\partial t}\left(\rho \sum_i Y_i h_i - p + \frac{\rho V^2}{2} \right) + \frac{\partial}{\partial x_j}\left[U_j \left(\rho \sum_i Y_i h_i + \frac{\rho V^2}{2} \right) \right] = \\ &\qquad \frac{\partial}{\partial x_j}\left[k \frac{\partial T}{\partial x_j} - \sum_i h_i \rho D_{i,m} \frac{\partial Y_i}{\partial x_j} + \tau_{ij} \cdot U_j - \rho \overline{h'_i u'_j} - \rho \overline{y'_i u'_j} - \rho \overline{u'_i u'_j} \cdot U_j \right] + S_h \end{aligned} \tag{6}$$

where h_i is the enthalpy for each chemical species i, τ_{ij} is the viscosity stress tensor and S_h is the source term that includes heat generated by other volumetric heat sources. The energy generated by combustion is already included in the mixture enthalpy, when a certain mass of reactants is transformed in products by chemical reaction. The enthalpy turbulent flux in Eq. (6) is modeled as:

$$-\rho \overline{h'_i u'_j} = \left(\alpha c_p \mu_{eff} - k \right) \frac{\partial T}{\partial x_i} \tag{7}$$

where μ_{eff} is the effective viscosity.

Using the RNG k-ε turbulent model, this viscosity can be written as:

$$\mu_{eff} = \mu + \rho C_{\mu} \frac{k^2}{\varepsilon} \tag{8}$$

The turbulent transport equations for kinetic energy k and dissipation rate ε are defined, respectively, as:

$$\frac{\partial \rho k}{\partial t} + \frac{\partial \rho U_i k}{\partial x_i} = \frac{\partial}{\partial x_j}\left[\left(\mu + \frac{\mu_t}{\sigma_k}\right)\frac{\partial k}{\partial x_j}\right] + \mu_t S^2 - \rho\varepsilon - 2\rho\varepsilon\frac{k}{\gamma RT} \tag{9}$$

$$\frac{\partial \rho \varepsilon}{\partial t} + \frac{\partial \rho U_i \varepsilon}{\partial x_i} = \frac{\partial}{\partial x_j}\left[\left(\mu + \frac{\mu_t}{\sigma_\varepsilon}\right)\frac{\partial \varepsilon}{\partial x_j}\right] + C_{1\varepsilon}\frac{\varepsilon}{k}\mu_t S^2 - C_{2\varepsilon}\rho\frac{\varepsilon^2}{k} \tag{10}$$

where σ_k, σ_ε, $C_{1\varepsilon}$ *and* $C_{2\varepsilon}$ are constants equal to 1.0, 1.3, 1.44 and 1.92, respectively. In Eq. (9) and (10), S is the module of the mean stress tensor, calculated by:

$$S = \sqrt{2 S_{ij} S_{ij}} \tag{11}$$

and μ_t is the turbulent viscosity, calculated by:

$$\mu_t = \rho C_{\mu} \frac{k^2}{\varepsilon} \tag{12}$$

where C_μ is a constant equal to 0.09.

The chemical reaction rate for species i is strongly non-linear and depends on local temperature and concentrations. To model the reaction rate, a chemistry-turbulence interaction mechanism is used and an average reaction rate is obtained. Here, the EDC (Eddy-Dissipation-Concept) model (Magnussen and Hjertager, 1976; Magnussen, 1981, 1989) is adopted. In this model, we assume that there is complete molecular mixing of reactants and products within the smallest turbulent scales, with dimensions proportional to the turbulent kinetic energy dissipation characteristic length scales (Kolmogorov scales). Within these small regions, called the inner region, there is a chemical reaction, controlled by a chemical reaction mechanism, transforming reactants to products. Here, the global one-step mechanism presented in Eq. 1 is used. Between the inner region and the outer region, there is reactants and products turbulent transport, controlled by the larger scales turbulent transport mechanisms. The local mass balance requires that the net mass flux of each chemical species i between both regions (in and out) is equal to the inner region chemical reaction rate.

In this model, the volumetric fraction of the flow occupied by turbulent smaller scales (inner region) is given by ξ^3 where ξ is defined by:

$$\xi = C_{\xi}\left(\frac{\nu\varepsilon}{k^2}\right)^{1/4} \tag{13}$$

where C_ξ is a volumetric fraction constant equal to 2.1377 and ν is the kinematic viscosity.

Mass renewal inside the small scales region occurs in a characteristic time given by:

$$\tau = C_{\tau}\left(\frac{\nu}{\varepsilon}\right)^{1/2} \tag{14}$$

where C_τ is a time scale constant equal to 0.4082.

The net mass flux between the inner and outer regions is given by:

$$R_i = \frac{\rho\xi^2}{\tau(1-\xi^3)}(Y_i^* - Y_i) \tag{15}$$

where Y_i^* is the mass fraction of chemical species i existing in the inner region. This model assumes one for the probability of reaction, denoted by χ in Magnussen (1981 and 1989) original work.

The inner region mass balance requires that the net mass flux be proportional to the molecular chemical reaction rate, which means

$$R_i^* = \frac{R_i}{\xi^3} \tag{16}$$

From the equation for the net mass flux, the mass and energy balances result in:

$$\frac{\rho^*}{\tau(1-\xi^3)}(Y_i^* - Y_i) = R_i^* \quad ; \quad \frac{\rho^*}{\tau(1-\xi^3)}(h^* - h) = q^* \tag{17}$$

where ρ^* is the mixture specific mass of small scales region and h^* and h are the mixture enthalpies of small scales and mean flow regions given by:

$$h^* = \sum_1^N Y_i^* h_i^* \; ; \qquad h = \sum_1^N Y_i h_i \tag{18}$$

where N is the number of chemical species present in the mixture (CH_4, O_2, N_2, H_2O and CO_2).
For the chemical reaction rate, the inner region can be modeled as a Perfectly Stirred Reactor (PSR). For a global mechanism reaction rate, we assume an Arrhenius model, given by:

$$R_i^* = \frac{M_i}{n_i}\left[AT^{\beta}\exp(-E/RT)\right]X_{CH_4}X_{O_2}^2 \tag{19}$$

where A is the pre-exponential factor, E is the activation energy, β is a temperature coefficient, R is the universal constant of gas, M_i is the molecular mass of chemical species i and n_i is the stoichiometric coefficient of chemical species i in Eq. (1).

The gas mixture is assumed to follow an ideal gas behavior, then,

$$p = \rho TR\sum_{i=1}^{N}\frac{Y_i}{M_i} \quad ; \quad h_i = h_{i,f}^o + \int_{T_o}^{T} c_{p,i}dT \quad ; \quad h_i^* = h_{i,f}^o + \int_{T_o}^{T^*} c_{p,i}dT \tag{20}$$

where $c_{p,i}$ is the specific heat of chemical species i and $h_{i,f}^o$ is the standard enthalpy of formation.

The system of equations valid in the small scales is solved for each control volume, in the form of a sub-grid model. From this solution, temperatures T^* and concentrations Y_i^* in the small scales region are obtained. This data, with local mass fraction Y_i, is then used to obtain the local average volumetric reaction rate from Eq. (15).

2.2. Boundary conditions

Boundary conditions for pressure, temperature, turbulent intensity and mixture composition must be defined. The inlet of intake system is set at: intake pressure of 101.3 kPa, temperature of 298 K, turbulent intensity of 3 % and stoichiometric mixture of dry air and methane (0.22026 oxygen mass fraction and 0.05507 methane mass fraction). The outlet of exhaust system is set at: exhaust pressure of 102.1 kPa, temperature of 523 K, turbulent intensity of 3 % and completely burned mixture (0.15143 carbon dioxide mass fraction and 0.12389 water vapor mass fraction).

Intake and exhaust system surfaces, as valve stem, were considered insulated. Otherwise, the surfaces of the combustion chamber were considered isothermal with temperature equal to 403 K.

The main engine working parameters for the base case are listed in Table 2. The effect of variations in ignition timing from 300 to 336 degrees will be tested. Each simulation starts with the piston in the top dead center and finishes 4 or 5 cycles later, when a periodic regime takes place.

Table 2. Main engine working parameters.

Engine speed	4,500 rpm	Intake valve close	224 CAD
Exhaust valve open	496 CAD*	Ignition energy	100 mJ
Exhaust valve close	720 CAD	Ignition duration	1.10^{-4} s
Intake valve open	0 CAD	Ignition timing	300 to 336 CAD

* CAD (crank angle degree)

3. NUMERICAL SOLUTION

The software Fluent v. 6.3.26 (2006) is used for the solution of the conservation equations. In this software, governing equations for mass, momentum, species, energy and turbulent quantities are solved using a finite volume methodology. For this, the computational domain is divided into finite volumes that are used to integrate the differential equations by Gauss Theorem in a collocated mesh arrangement.

The pressure-velocity coupling is solved by PISO formulation. In this finite volume method some proprieties need to be interpolated on finite volumes faces. Here, a second-order upwind scheme was adopted to solve mass, momentum, species and energy equations. Power-law scheme was adopted to solve turbulent quantities equations.

Under-relaxation factors equal to 0.6 were set for velocity fields, 0.3 was set for pressure, 0.7 was set for turbulent quantities and 0.95 was set to energy. Others quantities did not need under-relaxation factors. The solution was considered converged when the total residual was less than 10^{-3} for all the properties, except for the energy equation, for which the total residual should be less than 10^{-6}.

Since only long term periodic solutions are sought, the pressure fields for combustion chamber and intake system were initialized, respectively, with values of 102.1 kPa and 101.3 kPa respectively. Intake system initial temperature was set to 298 K, while combustion chamber and exhaust system initial temperatures were set to 700 K and 523 K, respectively. Intake system mass fractions were initialized with same values as stoichiometric air/methane mixture. Combustion chamber and exhaust system were initialized with same values as the total burned mixture.

The computational mesh has, approximately, 21,000 volumes at bottom dead center piston position and 6,000 volumes at top dead center piston position. Fig. 2 presents the computational mesh at bottom dead center position. Due to dynamic mesh grid refining, time step was limited to a maximum of 10^{-5} s.

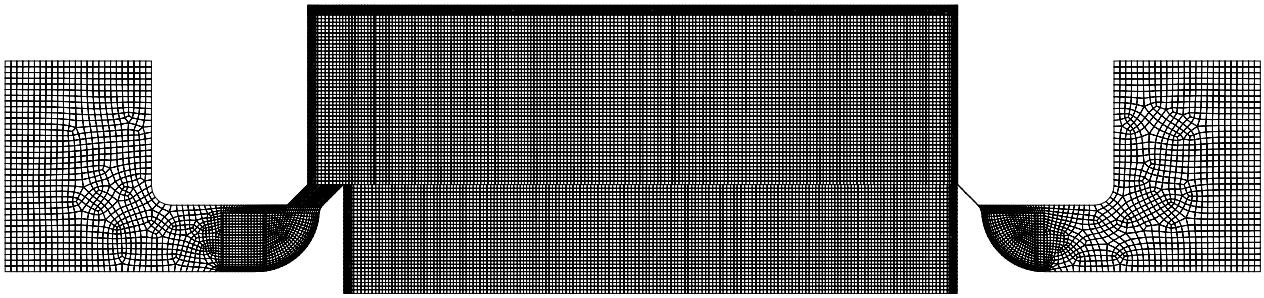

Figure 2. Mesh view at bottom dead center piston position.

4. RESULTS AND DISCUSSION

Initially, a baseline condition corresponding to the operating conditions represented in Table 2, with an ignition timing of 48 CAD BTDC, was studied. Figure 3 presents the in-cylinder pressure and temperature versus the crank angle for this condition. As can be seen, the form of the curve, for both pressure and temperature, resembles that for a typical internal combustion engine. The peak pressure obtained for this case is about 39.6 bar, whereas for temperature the maximum is about 2,100 K, which again are typical values expected for production engines.

The mass flow rates through the intake and exhaust valves are presented in Fig. 4. It can be observed that the highest mass flux at the intake valve occurs close to 110 degrees, which is the fully open valve position. However, the same does not happen for the discharge valve and, instead of happening at the maximum valve lift, the highest flow rate is seen at 540 degrees. This can be explained by the high level of the in-cylinder pressure when the exhaust valve opens, which creates a strong drive force for the flow (the blowdown period). The blowdown period is then followed by a scavenging period. The engine volumetric efficiency is found to be equal to 0.74 for the present situation. An interesting flow feature captured in the simulation is the backflow in the intake valve. The backflow at the beginning of the intake stroke is due to the higher pressure in the residual gas since the engine is throttled. The backflow at the end of the intake stroke is a consequence of the increased pressure inside the cylinder when the piston moves up towards the top dead center in the beginning of the compression stroke. For this engine speed, the inertia of the incoming flow was not large enough to overcome the small adverse pressure gradient.

The pressure-volume diagram in Fig. 5 shows that the pumping work is much less than the work delivered to the piston. The net work per cycle for this baseline engine is approximately equal to 334 J, with a thermal efficiency of 0.33.

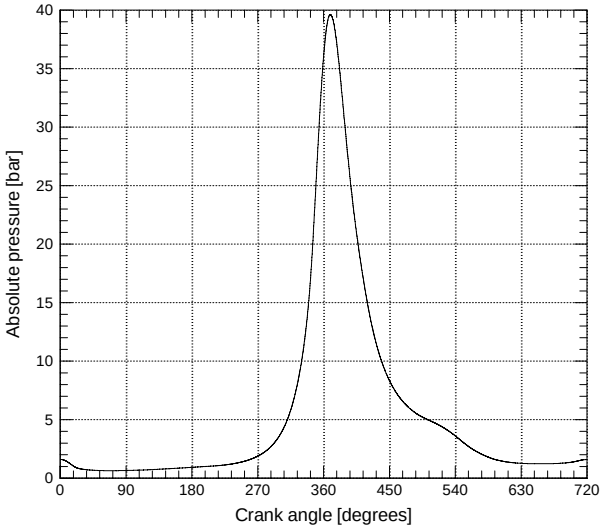

(a)

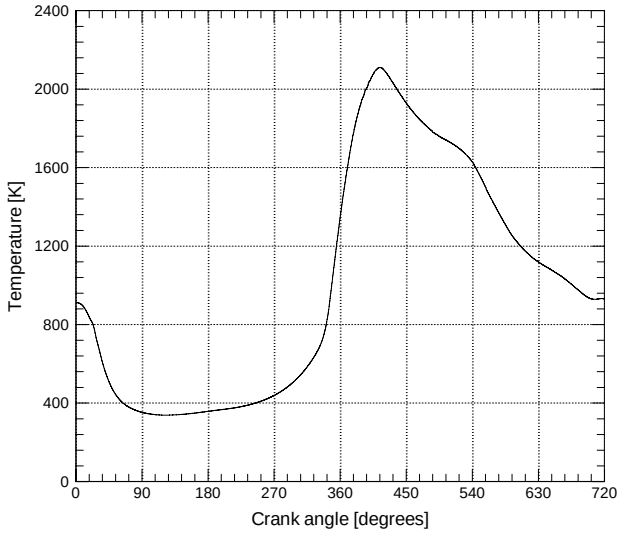

(b)

Figure 3. In-cylinder properties versus crank angle: (a) pressure; (b) temperature.

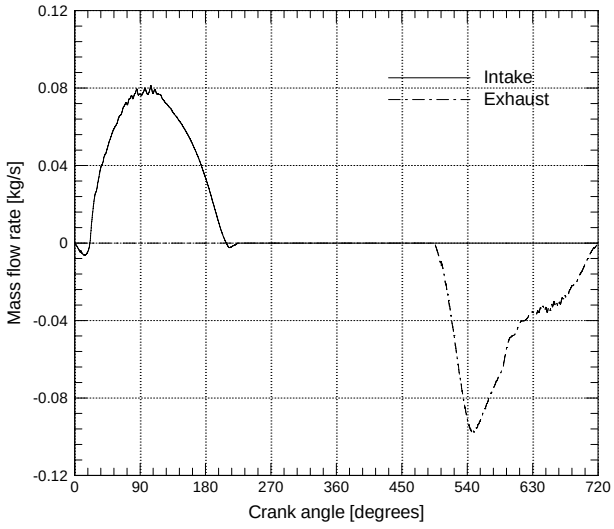

Figure 4. Mass flow rate through intake and exhaust valves versus crank angle.

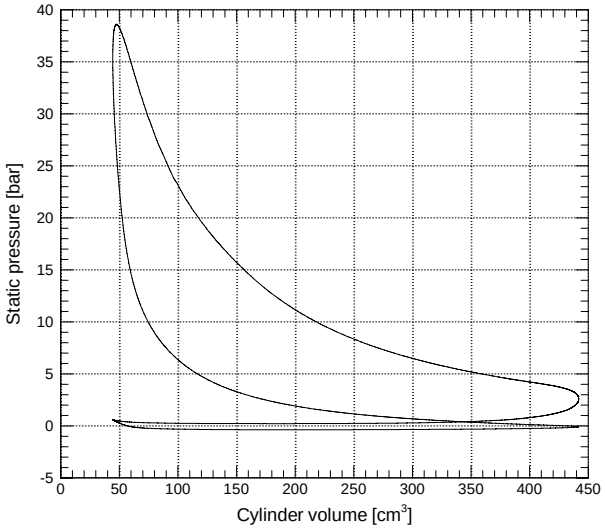

Figure 5. Pressure-volume diagram.

Figure 6 presents the combustion rate diagram, showing the oxygen and carbon dioxide in-cylinder averaged mass fraction versus the crank angle. According to Fig. 6, the duration of the overall burning process occurs between 312^o and 420^o, which means an overall burning angle of 108^o. This corresponds to the crank angle interval between the spark ignition and the end of the flame-propagation process (usually 90 % of mass fraction burned). After 520^o both mass fraction show a constant value until the end of the cycle. These constant values confirm that the combustion has ended. It can also be seen the steep increase in the oxygen mass fraction, and the consequent carbon dioxide mass fraction decrease, due to the air intake through the suction valve in the angle interval between 20^o and 90^o, approximately.

Temperature contours are shown in Fig. 7 for two crank angles: the first just after ignition timing, at 335^o, and the second at 345^o. From these results it is possible to analyze the flame front motion, which is a very important parameter to define the correct ignition timing, according to the selected fuel. During these 10^o of crank angle, the flame moves faster than the piston speed. The average front expansion speed of 17 m/s can be explained by the turbulence affected premixed flame propagation.

Figure 8 illustrates the turbulence intensity fields at two crank angles, corresponding to 60^o and 90^o. The turbulence intensity level has a fundamental role on the flame front propagation and can be adjusted by several techniques, such as modifications in the intake system and the combustion chamber geometry. An important aim of the induction system is to supply as much fresh air as possible to the cylinder and, at the same time, to establish a favorable flow pattern for the air/fuel mixing necessary in the subsequent combustion. Naturally, the precise characteristics of the resulting flow are dependent on the port/valve assembly, cylinder geometry and operating conditions.

The flow coming from the intake system exits the valve in a conic jet form, separating from both the valve and the valve seat surfaces. The interaction of the jet with the in-cylinder region results in large recirculating flow regions. On the other hand, the steep velocity gradients in the vicinity of the jet border generate most of the turbulence present in the cylinder during the induction stroke. Later, as the piston reaches the Bottom Dead Centre position (BDC), the jet starts losing momentum and, consequently, turbulence is reduced rapidly in the absence of stronger mean shear stresses.

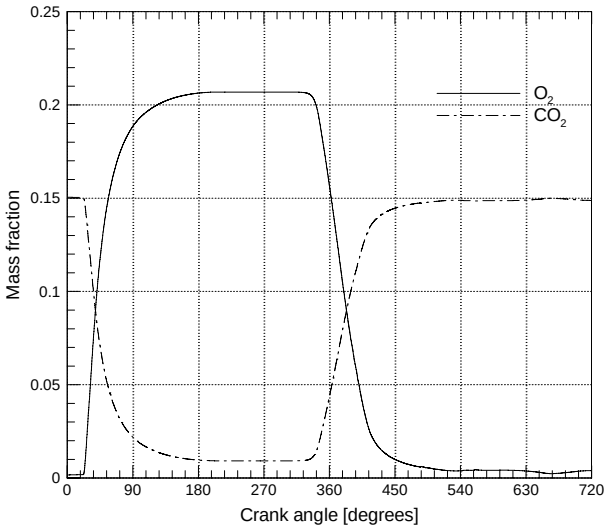

Figure 6. Combustion rate diagram.

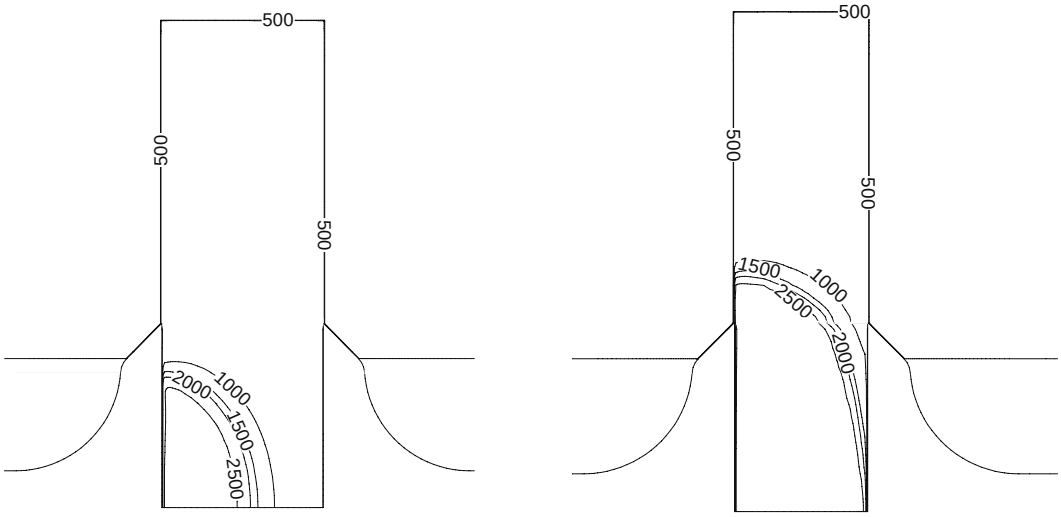

(a) (b)

Figure 7. Temperature [K] fields for two crank angles: (a) 335°; (b) 345°.

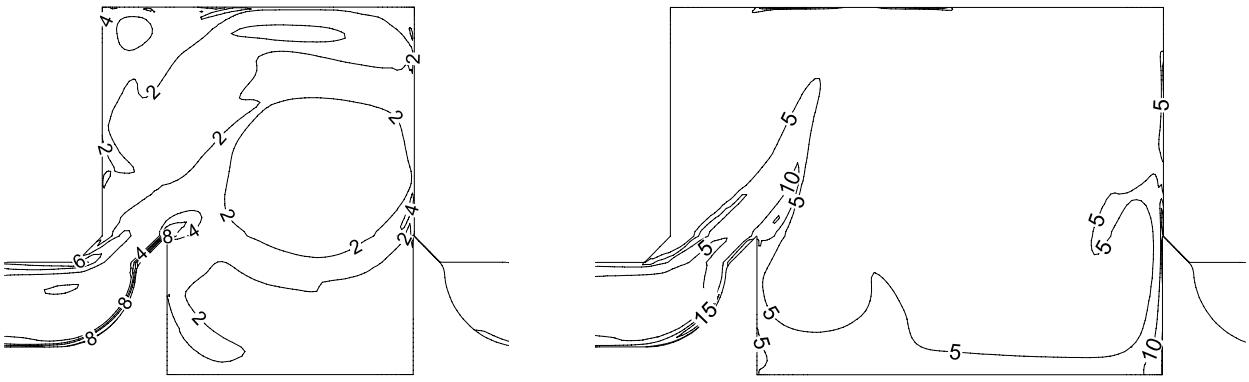

(a) (b)

Figure 8. Turbulence intensity fields for two crank angles: (a) 60°; (b) 90°.

After the intake valve is closed, the flow field inside the cylinder is the initial condition for the compression stroke. When the piston initiates its upward motion, the recirculating flow patterns from the induction process (swirl and tumble) are damped by pressure forces. Despite the highly non-homogeneous turbulence during the intake stroke, in the compression stroke this feature and also turbulence intensity are diminished. The flow field at the end of compression is of crucial importance, especially turbulence and mean velocity magnitudes close to the spark plug since flame propagation after ignition will be related to flow conditions there.

Usually the port/valve assembly is designed to produce a rotatory motion for the mixture inside the cylinder; commonly denominated swirl. It has been observed that during the compression stroke the swirling flow is not so affected by the pressure field as are other structures and that swirl can effectively speed up the combustion process although with some penalty to the valve discharge coefficient.

Finally, results for the engine performance are presented in Tab. 3 for six ignition timings. As can be seen, the engine performance is increased by the advance in the ignition timing. The worst performance is seen to occur at 24 CAD BTDC and can be explained by the low flame speed associated with the methane. For the engine speed considered (4,500 rpm), the low flame speed may cause the mixture not to burn completely before the exhaust valve is opened. As a consequence, a very small amount of work can be achieved from the combustion process.

The best performance obtained at 54 CAD BTDC ignition timing is again a result of synchronizing the methane flame speed with the piston motion. Because the ignition timing occurs very early, the mixture can be burned entirely in the chamber expansion. However, after this optimum condition, the engine starts decreasing its performance again, since if the ignition timing is too early an excessive compression work will occur due to the presence of burned mixture in the chamber.

Table 3. Engine performance according to ignition timing.

	Ignition Timing [CAD BTDC]						
	24	30	36	42	48	54	60
Volumetric Efficiency	0.72	0.72	0.74	0.74	0.74	0.74	0.74
Work [J]	152.97	192.58	248.50	306.18	334.52	346.80	289.97
Torque [kgf.m]	2.08	2.62	3.38	4.17	4.56	4.72	3.95
Power [hP]	7.80	9.82	12.67	15.61	17.06	17.68	14.78
Thermal Efficiency	0.15	0.19	0.24	0.30	0.33	0.34	0.28
Specific Fuel Consumption [g/kW.h]	466.44	374.34	293.62	238.66	219.96	211.63	252.29

5. CONCLUSION

The present paper considered the development of a two-dimensional numerical model to simulate a spark-ignition engine fuelled by a stoichiometric mixture of air and methane. The analysis revealed physical aspects related to the in-cylinder fluid dynamics, heat transfer and combustion, through results for temperature, pressure and turbulence intensity fields. The engine performance was assessed through predictions of indicated power, torque and specific fuel consumption, as well as volumetric and thermal efficiencies, for different ignition timing angles. The results were seen to be consistent with data of production engines. A next step in the research will consider a three-dimensional simulation of the engine, so that the influence of intake and exhaust systems can be included into the analysis. Moreover, the effect of turbulence on combustion and engine performance will also be explored.

6. ACKNOWLEDGEMENTS

The authors acknowledge the support received from CAPES (Coordination for the Improvement of High Level Personnel).

7. REFERENCES

Akansu, S.O., Dulger, Z., Kahraman, N. and Veziroglu, N., 2004, “Internal combustion engines fueled by natural gas – hydrogen mixtures”, International Journal of Hydrogen Energy, Vol. 29, pp. 1527-1539.

Cartellieri, W., Chmela, F.G., Kapus P.E. and Tatschl, R.M., 1994, “Mechanisms Leading to Stable and Efficient Combustion in Lean Burn Gas Engines”, COMODIA 94, Yokohama, pp. 17-24.

Das, L.M., Gulati, R. and Gupta, P.K., 2000, “A comparative evaluation of the performance characteristics of a spark ignition engine using hydrogen and compressed natural gas as alternative fuels”, Internal Journal of Hydrogen Energy, Vol. 25, pp. 783-793.

Fluent Inc., 2006, “FLUENT User's Guide”, v. 6.2.16, Lebanon/NH, USA.

Johansson, B. and Olsson, K., 1995, “Combustion Chambers for Natural Gas SI Engines Part I: Fluid Flow and Combustion”, SAE paper 950469.
Magnussen, B.F. and Hjertager, B.J., 1976, “On Mathematcal Modeling of Turbulent Combustion with Special Emphasis on Soot Formation and Combustion”, 16th Symp. (Int’l.) on Combustion, The Combustion Institute, Pittsburg, USA, pp.719-729.
Magnussen, B.F., 1981, “On the Structure of Turbulence and a Generalized Eddy Dissipation Concept for Chemical Reaction in Turbulent Flow”, 19th AIAA Aerospace Science Meeting, St.Louis, USA.
Magnussen, B.F., 1989, “Modeling of NOx and soot formation by the Eddy Dissipation Concept”, Int.Flame Research Foundation, 1st topic Oriented Technical Meeting, Amsterdam, Holland, 20 p.
Poinsot, T. e Veynante, D. , 2001, “Theoretical and Numerical Combustion”, R.T. Edwards, 490 p.
Thobois, L., Lauvergne, R., Gimbres, D. and Lendresse, Y., 2003, “The Analysis of Natural Gas Engine Combustion Specificities in Comparison with Isooctane Through CFD Computation”, SAE paper 2003-01-0009.
Weaver, C.S., 1989, “Natural gas vehicles – a part of the state of art”, SAE paper 892133.
Westbrook, C.K, Mizobuchi, Y., Poinsot, T.J., Smith, P.J. and Warnatz, J., 2005, “Computational combustion”, Proceedings of the Combustion Institute, Vol. 30, pp. 125-157.
Zhang, D. and Frankel, S.H., 1998, “A numerical study of natural gas combustion in a lean burn engine”, Fuel, Vol. 77, pp. 1339-1347.

8. RESPONSIBILITY NOTICE

The authors are the only responsible for the printed material included in this paper.